scientific reports

Check for updates

OPEN

Sustainable high-throughput microwell spectrophotometric methods for avapritinib quality control via charge-transfer complexation

Awadh M. Ali[1,5], Mohammed S. Alsalhi[1,5], Weam M. Othman[2]✉, Antonio Frontera[3], Waleed Alahmad[4] & Ibrahim A. Darwish[1]

Avapritinib (AVA) is a breakthrough targeted therapy as the first potent inhibitor approved for gastrointestinal stromal tumors (GIST) with PDGFRA D842V mutations. It lacks convenient analytical methods for routine quality control. This study addresses this gap by developing and validating two novel, green, high-throughput microwell spectrophotometric methods (MW-SPMs) for AVA quantification in pharmaceutical tablets—representing the first employment of charge-transfer complexation for AVA analysis. The methods exploit rapid charge-transfer complex (CTC) formation between AVA (electron donor) and two π-acceptors: 2,3-dichloro-5,6-dicyano-1,4-benzoquinone (DDQ) and chloranilic acid (CLA). The reactions, conducted in 96-well plates using only 200 µL total volume, yielded stable colored complexes with absorption maxima at 460 nm and 520 nm for the reactions with DDQ and CLA, respectively. Following ICH-compliant optimization and validation, both methods demonstrate excellent linearity (3.13–100 µg/well for DDQ; 6.25–100 µg/well for CLA), precision (RSD ≤ 1.8%), and accuracy (recoveries: 98.0–101.7%). Job's method confirmed 1:1 stoichiometry, while density functional theory (DFT) uniquely revealed the molecular basis for the stronger binding affinity of DDQ over CLA through dominant π–π stacking and hydrogen-bonding interactions, demonstrating how computational analysis can guide reagent selection in analytical method development. A comprehensive multi-metric sustainability assessment—utilizing ten tools including AES, AGREE, BAGI, RGB, and RAPI—confirmed the methods' excellent greenness (e.g., AES score = 90), superior practicality, and robust analytical performance, achieving a high White Index of 94.2%. With a substantially higher throughput of ~ 500 samples/hour and minimal solvent consumption (200µL/well), the proposed MW-SPMs offers a rapid, sustainable, and cost-effective alternative to conventional chromatographic and spectrofluorimetric techniques for routine pharmaceutical analysis, aligning with multiple United Nations Sustainable Development Goals.

Keywords Avapritinib, Charge-transfer complex, Microwell spectrophotometry, Green analytical chemistry, High-throughput analysis, Sustainability assessment, White analytical chemistry

Avapritinib (AVA) is a novel, potent, and highly selective type I tyrosine kinase inhibitor that targets mutant PDGFRA and KIT, particularly PDGFRA D842V and KIT D816V mutants that drive gastrointestinal stromal tumors (GIST) and systemic mastocytosis[1,2]. The chemical structure of AVA is given in Fig. 1, and it is chemically named as: (1S)-1-(4-fluorophenyl)-1-(2-{4-[6-(1-methyl-1H-pyrazol-4-yl)pyrrolo[1-f]triazin-4-yl]piperazin-1-yl}pyrimidin-5-yl)ethanamine. It is approved for the treatment of adults with unresectable or metastatic GIST harboring PDGFRA exon 18 mutations and for advanced forms of aggressive systemic mastocytosis,

[1]Department of Pharmaceutical Chemistry, College of Pharmacy, King Saud University, P.O. Box 2457, 11451 Riyadh, Saudi Arabia. [2]Pharmaceutical Analytical Chemistry Department, Faculty of Pharmacy, Misr University for Science and Technology, 6Th October City, Egypt. [3]Department de Química, Universitat de Les Illes Balears, Crta. de Valldemossa Km 7.5, 07122 Palma, Spain. [4]Department of Chemistry, Faculty of Science, Chulalongkorn University, Bangkok 10330, Thailand. [5]Awadh M. Ali and Mohammed S. Alsalhi contributed equally to this work. ✉email: Weam.mahmoud@must.edu.eg; Dr.weamelfergan@gmail.com

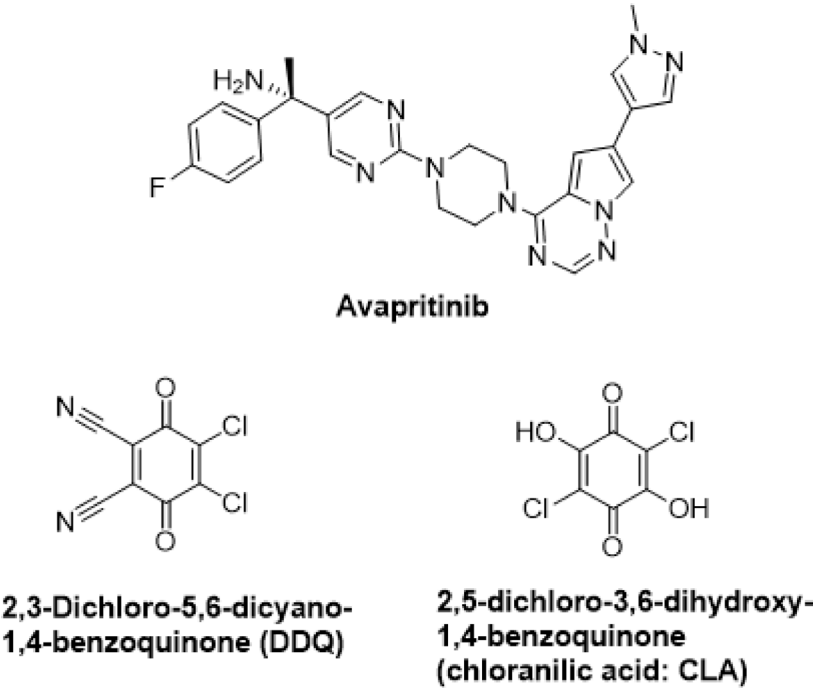

Fig. 1. The chemical structures of Avapritinib (AVA), 2,3-dichloro-5,6-dicyano-p-benzoquinone (DDQ) and 2,5-chloro-3,6-dihydroxy-1,4-benzoquinone (chloranilic acid: CLA).

representing a paradigm shift and reflecting a pivotal role in the management of these otherwise refractory malignancies[1,2]. AVA possesses high lipophilicity (log P ~ 3.5) and poor aqueous solubility, characteristics that necessitate reliable analytical methods for quality control of its solid dosage forms[1,2]. AVA is marketed under the trade name of AYVAKIT™ tablets for oral use, manufactured by Blueprint Medicines Corporation (Cambridge, MA, USA)[3]. Despite its clinical success, AVA's efficacy is hindered by a narrow therapeutic index, necessitating careful dose management to balance its potent anticancer effects against the risk of significant adverse effects[3]. The narrow therapeutic index and chronic therapy of AVA necessitate rigorous, reliable, and sustainable quality control (QC) methods for its dosage forms.

Existing analytical methods for AVA include chromatographic techniques such as HPLC-UV[4–10]and UPLC-MS/MS[11–13]. Although these methods offer high sensitivity and selectivity, they require sophisticated instrumentation, long analysis times, and multistep sample preparation, which are laborious for routine QC laboratories. Spectrofluorimetric methods using derivatization[14–16] or micelle enhancement[17]have also been reported, but they involve time-consuming, temperature-controlled reaction steps and introduce variables that limit robustness and reproducibility. These methods consume considerable volumes of organic solvents and generate significant chemical waste, conflicting with Green Analytical Chemistry (GAC) principles[18,19]. While acetonitrile is not a green solvent by strict standards, the miniaturized method (200 µL /well) drastically reduces solvent consumption and waste, which is the primary contributor to its overall greenness. Several charge-transfer based spectrophotometric methods have been reported for related pharmaceutical compounds, demonstrating the utility of π-acceptor reagents for analytical applications[20–22]. Therefore, a simpler, faster, and inherently parallel alternative is needed.

Driven by GAC concepts, recent trends prioritize methods that minimize solvent consumption, reduce hazardous waste, and lower energy requirements while maintaining analytical performance suitable for QC[21,22]. Additionally, high-throughput strategies that allow the simultaneous or parallel processing of large numbers of samples are increasingly adopted to improve productivity and reduce per-sample cost in pharmaceutical QC laboratories[23,24].

Microwell-based methods using 96-well plates have emerged as attractive platforms that naturally integrate green and high-throughput features[25,26]and have been successfully applied for drug quantification in dosage forms[27–29]. Microwell spectrophotometric methods (MW-SPMs) employ microplates and absorbance readers to measure multiple samples in parallel using micro-volumes of sample solutions and reagents, leading to reduced solvent consumption and minimal waste generation. The batch-wise nature of plate-based measurements markedly increases analytical throughput compared with conventional cuvette-based spectrophotometry and chromatographic techniques, enabling rapid processing of large sample sets. Furthermore, MW-SPMs are operationally simple and rely on widely available microplate readers, making them cost-effective and readily adaptable in pharmaceutical QC laboratories[27–29].

Charge-transfer (CT) reactions between electron-donating drugs and π-acceptor reagents provide intensely colored complexes suitable for spectrophotometric method development[30–32]. These CT-based methods are simple, rapid, and rely on inexpensive, commonly available reagents, allowing facile implementation without

complex instrumentation. When integrated into microwell formats, CT reactions combine the advantages of simple procedures and sensitive colorimetric detection with green and high-throughput characteristics[33–35].

The present work advances the field in three distinct ways. First, it represents the first CT-based MW-SPM for AVA, leaving a gap in simple, high-throughput QC platforms. Second, this study provides the first multi-metric assessment of a CTC method using ten complementary indices (AES, AGREE, MoGAPI, BAGI, CACI, RGB, AGSA, CaFRI, VIGI, RAPI), establishing a benchmark for holistic method evaluation. Third, by correlating experimental binding parameters with DFT-calculated interaction energies and NCI plots, the study offers a molecular level of mechanistic insight on the CT complexation reaction. Consequently, the present study investigates the CT complexation of AVA with DDQ and chloranilic acid (CLA) and exploits these reactions for the development and validation of novel MW-SPMs for AVA determination in pharmaceutical tablets. DDQ and CLA were selected for their well-established roles as efficient electron acceptors in CT complexation[36,37]. DDQ is renowned for its high electron affinity, forming stable, deeply colored complexes with high molar absorptivity[36,37]. Conversely, CLA offers excellent reactivity under milder conditions and has been successfully integrated into modern high-throughput and green analytical platforms[37,38]. Both reagents are commercially available, inexpensive, and have a proven history in developing reliable spectrophotometric methods[36–38]. Their selection allows a comprehensive investigation of AVA's CT reactivity and the development of optimized MW-SPMs, providing a green, rapid, and analytically robust alternative for QC laboratories.

Experimental

Apparatus

A double-beam, ultraviolet-visible spectrophotometer (UV-1800: Shimadzu Corporation, Kyoto, Japan) with 1-cm quartz cells was used. An absorbance microplate reader (ELx808: Bio-Tek Instruments Inc., Winooski, USA) controlled with KC Junior software, provided with the instrument, was utilized for microwell-based analysis.

Chemicals and materials

Avapritinib (AVA), with purity of ≥ 99%, was obtained from Hangzhou Leap Chem Co., Ltd. (Hangzhou, Zhejiang, China). DDQ and CLA were purchased from Sigma-Aldrich Chemicals Co. (St. Louis, MO, USA). Laboratory-made AVA Tablets were prepared to contain 50 mg AVA per tablets. The tablets contained inactive ingredients (copovidone, croscarmellose sodium, magnesium stearate, and microcrystalline cellulose), and tablet coating substances polyethylene glycol, polyvinyl alcohol, talc, and titanium dioxide) according to the composition of the commercial AYVAKIT™ 50 mg tablets as per the FDA prescribing information[3]. Corning® 96-well transparent assay plates were acquired from Merck & Co. (Rahway, New Jersey, NJ, USA). Acetonitrile (HPLC grade) and methanol (HPLC grade) were obtained from Fisher Scientific (California, CA, USA).

Preparation of standard AVA solutions

AVA stock solution (1 $mgmL^{-1}$) was prepared by dissolving 10 mg of AVA in 10 mL acetonitrile. This stock solution was diluted with acetonitrile to acquire working solutions of AVA with concentrations suitable for the corresponding experiments. Acetonitrile was selected as the solvent for all experiments based on its excellent solubilizing properties for AVA and its compatibility with the charge-transfer complexation reactions.

Preparation of tablets sample solution

To obtain tablet samples for analysis, a measured amount of the lab-made tablets powder, equivalent to 25 mg of AVA, was placed into a 25-mL volumetric flask. About 15 mL of acetonitrile was added, and the mixture was shaken vigorously to ensure the complete dissolution of AVA in acetonitrile and separated from the tablet excipients. The solution was filtered, and the filtrate was diluted with acetonitrile to obtain AVA solutions with concentrations ranging from 100 to 800 μgmL^{-1}. These solutions were subjected to analysis for their respective AVA concentrations using the proposed MW-SPMs.

Determination of association constants

A series of AVA solutions containing varying concentrations (5.0×10^{-5}– 5.5×10^{-4} M) were prepared in acetonitrile. Each of these solutions reacted with a fixed concentration of DDQ (5.5×10^{-3} M) and CLA (6.0×10^{-3} M) for ~ 5 min at room temperature (25 ± 2 ℃). The absorbances of the reaction mixtures were measured, and the measured absorbances were utilized to construct the Benesi-Hildebrand plots[39]. The plot establishes a relationship between 1/[D] and [A]/A, where [D], [A], and A represent the molar concentration of AVA, molar concentration of acceptor (DDQ and CLA), and absorbance of the complex, respectively. Regression statistical analysis was conducted on the data, and the obtained results were used for calculating the association constants of the CTCs.

Determination of reaction stoichiometry

The Job's method[40] was employed for the determination of stoichiometry of CTCs of AVA with both DDQ and CLA. Equimolar solutions (4.0×10^{-3} M) of both AVA and acceptors were prepared. Varying volumes (in µL) of AVA and each of DDQ and CLA solutions were mixed in the microwells of the assay plate to make up different complementary volumes of AVA:acceptor (0:200, 25:175, 50:150, …… 150:50, 175:25, 200:0). The absorbances of each reaction mixture was measured and plotted as a function of mole fraction of AVA. The generated Job's plots were used to determine the stoichiometry of the reactions between AVA with DDQ and CLA.

Computational analysis

The density functional theory (DFT) calculations were carried out using the Gaussian-16 software package[41]. The geometries of the isolated monomers (AVA, CLA, and DDQ) were fully optimized without imposing any symmetry constraints at the PBE0-D3/def2-TZVP level of theory[42–44]. This functional includes Grimme's D3 dispersion correction[46], which is essential for accurately describing non-covalent interactions in these systems. To identify the most favorable binding modes for the 1:1 charge transfer complexes, a conformational search was first performed using the CREST code (Conformer-Rotamer Ensemble Sampling Tool, version 2.12) with its default settings[45]. This exploration of the potential energy surface allowed for the identification of the most likely association geometries. The most stable structures obtained from CREST were subsequently re-optimized in Gaussian-16 at the PBE0-D3/def2-SVP level of theory[42–44]. The def2-TZVP basis set was used for the initial optimization of monomers to ensure high accuracy in electronic properties. For the subsequent optimization of the 1:1 complexes, the def2-SVP basis set was employed as a compromise between computational cost and accuracy, as it provides reliable geometries for non-covalent interactions while being computationally less demanding for the larger complex systems. This two-step approach is widely accepted in DFT studies of charge-transfer complexes.

The binding energies for the complexes were calculated as the difference between the energy of the optimized complex and the sum of the energies of the isolated monomers. These values were corrected for the Basis Set Superposition Error (BSSE) using the counterpoise method[46]. Finally, the nature of the intermolecular interactions was characterized using the Non-Covalent Interaction (NCI plot) index[47], which was computed using the AIM All program[48] to generate the reduced density gradient (RDG) isosurfaces.

Procedures of MW-SPMs

Aliquots (100 µL) of AVA standard solution containing various concentrations of AVA in the ranges of31.3–1000and 62.5–1000 $\mu g mL^{-1}$ (for DDQ and CLA, respectively) were dispensed into wells of an assay plate. Subsequently, 100 µL of a 1.0% (w/v) of either DDQ or CLA solution was added to each well, and the reaction was allowed to proceed for 5 min at room temperature (25 ± 2 °C). The absorbance of the solutions in each well was then measured using an absorbance microplate reader at 460 and 520 nm for analysis by DDQ and CLA, respectively.

Comprehensive sustainability and performance assessment

A multifaceted assessment strategy was employed to holistically evaluate the environmental sustainability, analytical performance, and operational practicality of the MW-SPMs. Ten distinct metric tools were applied, the implementation of which is detailed in the following subsections.

Analytical Eco-Scale

The Analytical Eco-Scale (AES)[49] is a semi-quantitative tool that evaluates environmental impact through a penalty point system. Starting from an ideal baseline score of 100, points are deducted for negative environmental and safety attributes across four principal categories: (1) the quantity and toxicity of reagents, (2) the energy consumption of equipment, (3) occupational hazards, and (4) waste generation. The final score is interpreted as follows: > 75 indicates an excellent green method, 50–75 signifies acceptable greenness, and < 50 denotes an insufficiently green procedure. This approach yields a transparent numerical output, enabling straightforward comparison between analytical methods.

Analytical GREEnness

The Analytical GREEnness (AGREE)[50] is a software-supported tool that provides a quantitative and visual assessment based on the twelve principles of Green Analytical Chemistry (GAC). Each principle—encompassing sample preparation, scale, device location, integration, automation, derivatization, waste, throughput, energy, renewable sources, reagent toxicity, and operator safety—is weighted according to its contextual importance. The software generates a score between 0 and 1, accompanied by a color-coded, clock-style pictogram that offers an immediate visual summary of the method's greenness profile.

Modified green analytical procedure index

The Modified Green Analytical Procedure Index (MoGAPI)[51] represents an evolution of the original GAPI tool, offering a more quantitative evaluation of an analytical method's lifecycle from sampling to waste disposal. It assesses 15 distinct criteria, presented in a multi-section pictogram. A unique feature of MoGAPI is its integrated assessment of "Whiteness," which synthesizes greenness (environmental impact), redness (analytical performance), and blueness (practicality). A final score of 75% or higher corresponds to an "Excellent Green" procedure.

Blue applicability grade index

The Blue Applicability Grade Index (BAGI)[52] was used to quantify the practical utility and feasibility of the developed assay, focusing on the "Blue" dimension of White Analytical Chemistry (WAC). This index evaluates ten key practical attributes, including analysis type, number of analytes, throughput, reagent types, instrument requirements, batch size, need for preconcentration, automation level, sample preparation format, and sample amount. The resulting score and pictogram indicate the method's suitability for routine application across diverse laboratory environments.

Click analytical chemistry index

Inspired by the concepts of "click chemistry," the Click Analytical Chemistry Index (CACI)[53] evaluates the simplicity, efficiency, and robustness of an analytical procedure. It assesses 12 criteria related to sample handling, sensitivity, cost, and accessibility. The results are visualized in a color-coded hexagonal pictogram, and a cumulative percentage score is calculated, with higher values denoting more modular, user-friendly, and reliable analytical workflows.

Red–green–blue model

The Red–Green–Blue (RGB) model[54] is a White Analytical Chemistry (WAC) framework designed to balance three critical aspects: ecological safety (Green), analytical performance (Red), and practical applicability (Blue). The ideal method achieves a harmonious equilibrium, represented as a "whiteness" score. A perfectly optimized method, scoring 100% in all three categories, is visualized as pure white, ensuring that environmental goals do not compromise analytical rigor or practical feasibility.

Analytical green star area

The Analytical Green Star Area (AGSA)[55] provides a geometric quantification of greenness based on the 12 GAC principles. Each principle corresponds to a vertex on a dodecagonal (12-sided) star-shaped profile. The AGSA index is calculated as the ratio of the area of the generated polygon to the maximum possible area. This approach translates qualitative principles into a precise quantitative metric, where a larger star area indicates a superior sustainability profile.

Carbon footprint reduction index

The Carbon Footprint Reduction Index (CaFRI)[56] is a software-aided metric that specifically evaluates a method's impact on greenhouse gas emissions. It assesses direct and indirect carbon contributions across five categories: (1) sample storage, (2) transportation, (3) reagent consumption, (4) energy efficiency, and (5) waste treatment. Parameters are rated using CO_2 emission factors, culminating in a final CaFRI score that quantifies the carbon reduction effectiveness of the analytical protocol.

Violet innovation grade index

The Violet Innovation Grade Index (VIGI)[57] is a pioneering, survey-based tool designed to evaluate the innovativeness of an analytical method. It assesses ten criteria, including miniaturization, automation, and interdisciplinary contribution. The results are presented in a star-shaped decagon pictogram, visually highlighting areas where the method provides significant scientific advancement. This ensures that the assessed procedure is not only sustainable but also contributes novel value to the field.

Red analytical performance index

The Red Analytical Performance Index (RAPI)[58] is a dedicated software tool that quantitatively evaluates the "Red" (performance) component of the RGB model. It focuses on ten key validation parameters: sensitivity, linear range, precision, accuracy, selectivity, robustness, stability, recovery, throughput, and simplicity. Each parameter is scored from 0 to 1, and the composite result is displayed in a circular pictogram where the cumulative area of the red segments provides a visual and quantitative representation of the method's analytical quality.

Results and discussion

Reactions and absorption spectra

The UV–Vis spectrum of pure AVA in acetonitrile showed a strong characteristic peak at 260 nm, corresponding to the π–π* transition of its aromatic system (Fig. 2A). Upon reaction with the π-acceptors DDQ and CLA, the colorless AVA solutions developed intense visible colors. The reaction with DDQ produced a red solution with a maximum absorption at 460 nm (Fig. 2B), while the reaction with CLA yielded a violet solution with a maximum at 520 nm (Fig. 2C). The absorbance at these wavelengths increased linearly with AVA concentration at fixed acceptor concentration, confirming the formation of well-defined charge-transfer complexes (CTCs). These distinct, stable absorption bands in the visible region are consistent with the formation of radical-anion complexes typical of DDQ and CLA with electron-donating drugs. The use of acetonitrile as a solvent effectively stabilized these complexes, facilitating straightforward and reproducible spectrophotometric monitoring[37]. Although AVA alone exhibits a strong UV absorption peak at 260 nm (Fig. 2A), complexation with DDQ or CLA offers distinct advantages for pharmaceutical quality control. First, the UV region is prone to interference from common tablet excipients (e.g., microcrystalline cellulose, croscarmellose sodium) and UV-absorbing impurities, whereas the visible region (460 nm and 520 nm) is typically interference-free, enhancing selectivity. Second, the development of intense visible colors (red for DDQ, violet for CLA) allows for visual inspection and enables high-throughput microwell plate reading without specialized UV detection equipment. Thus, the charge-transfer complexation transforms the analytical signal from a non-specific UV region to a highly selective visible region, which is particularly advantageous for routine QC laboratories.

The proposed charge-transfer complexation involves electron donation from the electron-rich pyrrolotriazine moiety of AVA (donor) to the π-accepting rings of DDQ or CLA (acceptors). This one-electron transfer process forms colored radical-anion complexes: $AVA^{+}\bullet$–$DDQ^{-}\bullet$ (red, λ_{max} = 460 nm) and $AVA^{+}\bullet$–$CLA^{-}\bullet$ (violet, λ_{max} = 520 nm). The reaction can be summarized as: AVA (donor) + DDQ/CLA (acceptor) → [$AVA^{+}\bullet$ – $DDQ^{-}\bullet$/$CLA^{-}\bullet$] colored complex.

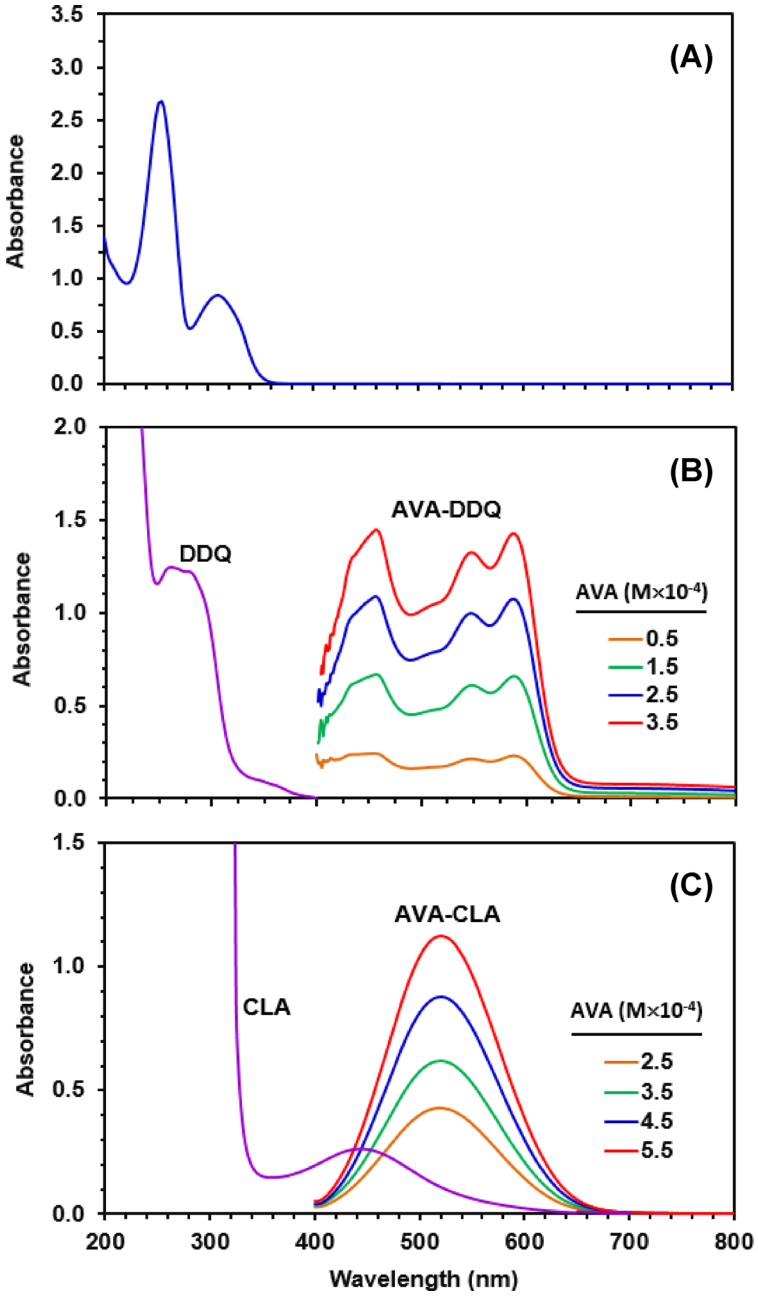

Fig. 2. Panel (**A**): the absorption spectra of AVA (5.0×10^{-5} M). Panel (**B**): the absorption spectra of DDQ (1.4×10^{-3} M) and its reaction solutions (AVA-DDQ) with varying concentrations of AVA (0.5×10^{-4}–3.5×10^{-4} M). Panel (**C**): the absorption spectra of CLA (1.0×10^{-3} M) and its reaction solutions (AVA-CLA) with varying concentrations of AVA (2.5×10^{-4}–5.5×10^{-4} M). All solutions were prepared in acetonitrile.

Characteristics of AVA CTCs

The electronic properties of the formed CTCs were evaluated. The optical band gap energies (Eg), determined from Tauc plots (Fig. 3A), were 2.72 eV for AVA–DDQ and 2.39 eV for AVA–CLA (Table 1). These relatively low-energy gaps indicate efficient charge transfer under visible light excitation. The complexes exhibited substantial molar absorptivity (ε), with AVA–DDQ showing higher sensitivity (1.39×10^3 L mol^{-1} cm^{-1}) compared to AVA–CLA (8.27×10^2 L mol^{-1} cm^{-1}) (Table 1). The association constants (*K*), derived from the Benesi–Hildebrand plots (Fig. 3B), were determined to be 6.5×10^2 L mol^{-1} for AVA–DDQ and 3.77×10^2 L mol^{-1} for AVA–CLA (Table 1). The negative Gibbs free energy values (– 16.05 and – 14.70 kJ mol^{-1} for DDQ and CLA, respectively) confirm the spontaneous nature of the complexation. Additional parameters, including oscillator strength and resonance energy, further support the stability and pronounced CTCs characters (Table 1).

The stoichiometry of the reactions was unequivocally determined to be 1:1 (AVA:acceptor) using Job's method of continuous variation. The Job's plots for both acceptors displayed clear maxima at a mole fraction of

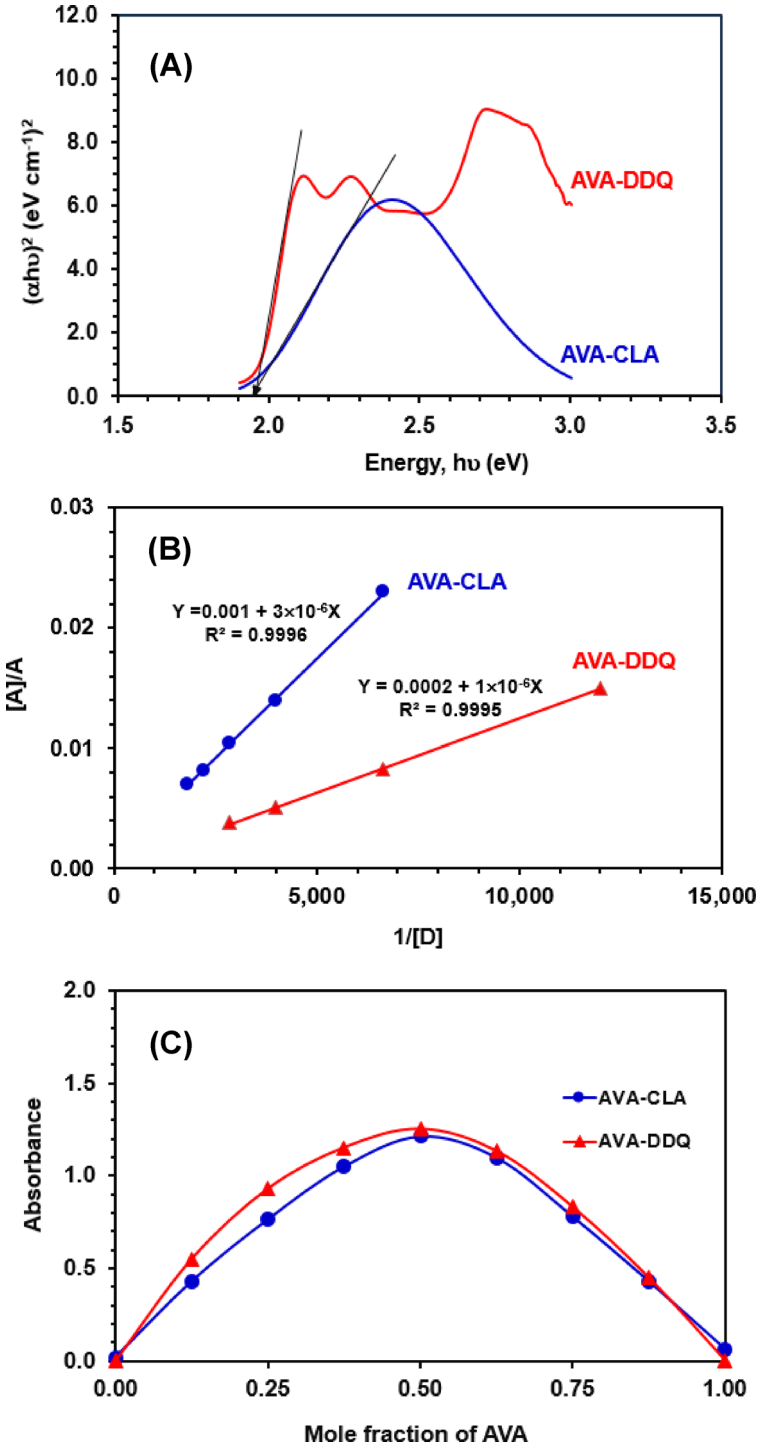

Fig. 3. Panel (**A**): The Tauc plots of energy (hυ) against Kubelka–Munk function $(\alpha h\upsilon)^2$ for CTCs of AVA with DDQ and CLA. All solutions were prepared in acetonitrile. Panel (**B**): The Benesi–Hildebrand plots for the formation of the CTCs of AVA with CLA (Blue circle) and DDQ (Red triangle). Linear fitting equations and their determination coefficients (R^2) are given on the plots. [A], A, and [D] are the molar concentration of the acceptor reagent (CLA or DDQ), the absorbance of the CTC, and molar concentration of AVA, respectively. Panel (**C**): The Job's plots for determination of the stoichiometry of CTCs of AVA with CLA (Blue circle) and DDQ (Red triangle).

Parameters	AVA-DDQ	AVA-CLA
Wavelength, nm	460	520
Molar coefficient (ε), L mol^{-1} Cm^{-1}	1.39×10^3	8.27×10^2
Association constant (K), L mol^{-1}	6.5×10^2	3.77×10^2
Oscillator strength (*f*)	0.97	0.58
Transition dipole moment (μ, Debye)	0.25	0.15
Ionization potential (Ip), eV	9.11	8.70
Energy (hυ), eV	2.72	2.39
Resonance energy (RN), eV	0.03	0.02
Dissociation energy (W), eV	3.69	5.21
Gibbs free energy (ΔG°), kJ $mole^{-1}$	− 16.05	− 14.70

Table 1. Spectroscopic and electronic parameters for CTCs of AVA with DDQ and CLA.

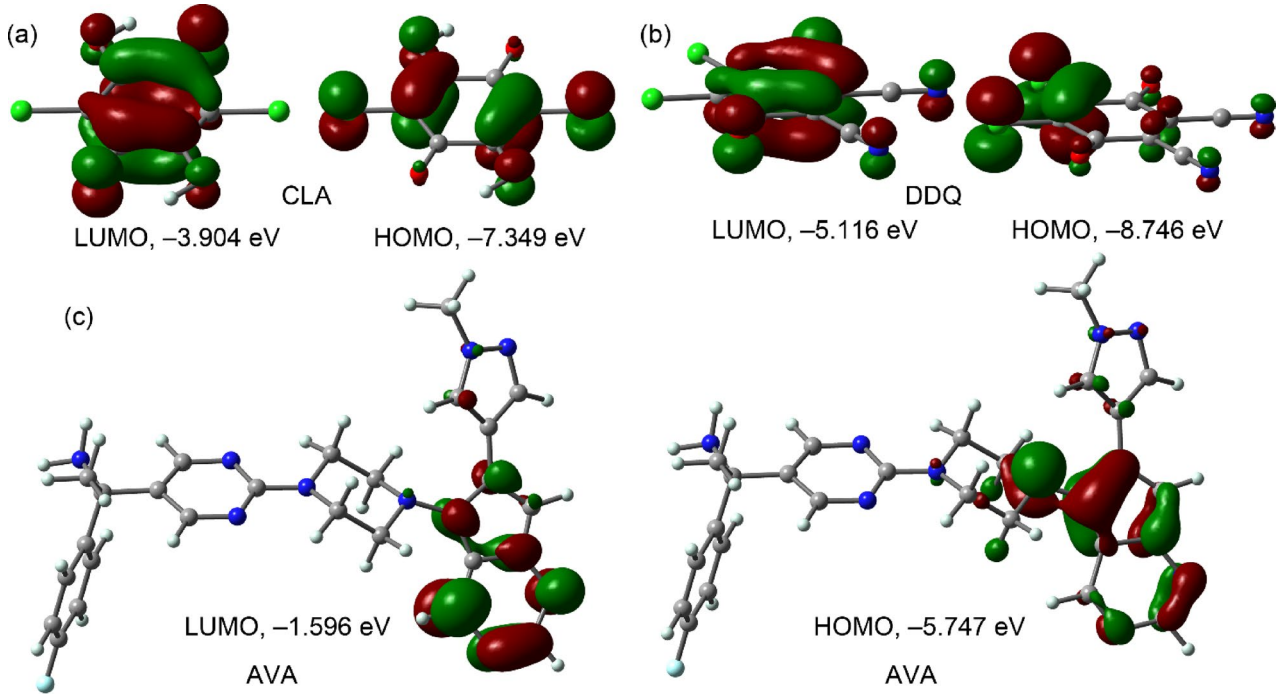

Fig. 4. Frontier Molecular Orbitals (FMOs) of the reactant species calculated at the PBE0-D3/def2-TZVP level of theory. The spatial distribution and orbital energies (in eV) of the Highest Occupied Molecular Orbital (HOMO) and Lowest Unoccupied Molecular Orbital (LUMO) are presented for (**a**) CLA, (**b**) DDQ, and (**c**) AVA.

0.5 (Fig. 3C). This finding provides the fundamental stoichiometric basis for the quantitative analytical methods developed in this study.

Density functional theory computational study

To provide a molecular-level interpretation of the experimental spectrophotometric data, which indicated the formation of 1:1 stoichiometric complexes, we performed a comprehensive computational analysis using Density Functional Theory (DFT). The computational workflow commenced with an analysis of the Frontier Molecular Orbitals (FMOs) of the isolated monomers to assess their global reactivity and donor–acceptor capabilities. Following this electronic characterization, an extensive conformational search was conducted using the NCI-CREST code to sample the potential energy surface for the 1:1 association. The most stable conformers identified were subsequently re-optimized at the PBE0-D3/def2-SVP level of theory to characterize the structural and energetic properties of the complexes.

The reactivity of the interacting species was first assessed by analyzing their Frontier Molecular Orbitals (FMOs). Figure 4 displays the HOMO and LUMO distributions for the isolated reactants optimized at the PBE0-D3/def2-TZVP level of theory. As shown in Fig. 4a, b, the FMOs of the acceptors (CLA and DDQ) are π-type orbitals predominantly delocalized over the six-membered rings and their attached substituents. In contrast, the orbitals of the donor AVA (Fig. 4c) are largely localized on the electron-rich pyrrolotriazine moiety.

The calculated orbital energies confirm the electronic character of these compounds. Both CLA and DDQ exhibit low LUMO energies (−3.904 eV and −5.116 eV, respectively), indicating a strong capacity to accept electrons. Conversely, AVA presents a high HOMO energy (−5.747 eV), consistent with its role as an electron donor. Notably, the energy gap between the LUMO of DDQ and the HOMO of AVA is significantly narrower than the corresponding gap for CLA. This suggests that electron transfer from AVA to DDQ is energetically more favorable and is expected to occur more readily than the transfer to CLA.

Following the FMO analysis, Molecular Electrostatic Potential (MEP) surfaces were generated to identify the most likely electrophilic and nucleophilic sites on the reactants, thereby predicting potential regions for intermolecular interaction. As presented in Fig. 5a, b, both electron acceptors, CLA and DDQ, exhibit significant positive electrostatic potential (blue regions) above and below the plane of their six-membered rings. This feature confirms their nature as π-acidic rings appropriate for stacking interactions with electron-rich systems. For DDQ, a strong local MEP maximum of + 42.7 kcal/mol is located directly over the quinone ring center. In the case of CLA, while the ring center is positive (+ 26.4 kcal/mol), the global MEP maximum (+ 44.6 kcal/mol) is localized on the hydrogen atoms of the hydroxyl groups, indicating their potential to act as strong hydrogen bond donors.

The MEP surface of the donor molecule, AVA, is shown in Fig. 5c. The surface reveals distinct regions of negative potential (red), indicative of electron-rich sites suitable for electrophilic attack or H-bond acceptance. The global MEP minimum (−33.8 kcal/mol) is located at a nitrogen atom of the terminal pyrrolotriazine moiety, confirming the electron-donating character originating from this part of the molecule. Significant negative potentials are also observed near the nitrogen atoms of the central pyrazine ring (− 19.5 and − 18.5 kcal/mol). Conversely, an MEP maximum of + 32.7 kcal/mol is found at the hydrogens of the amino ($-NH_2$) group attached to the pyrazine ring, highlighting its ability to act as a hydrogen bond donor.

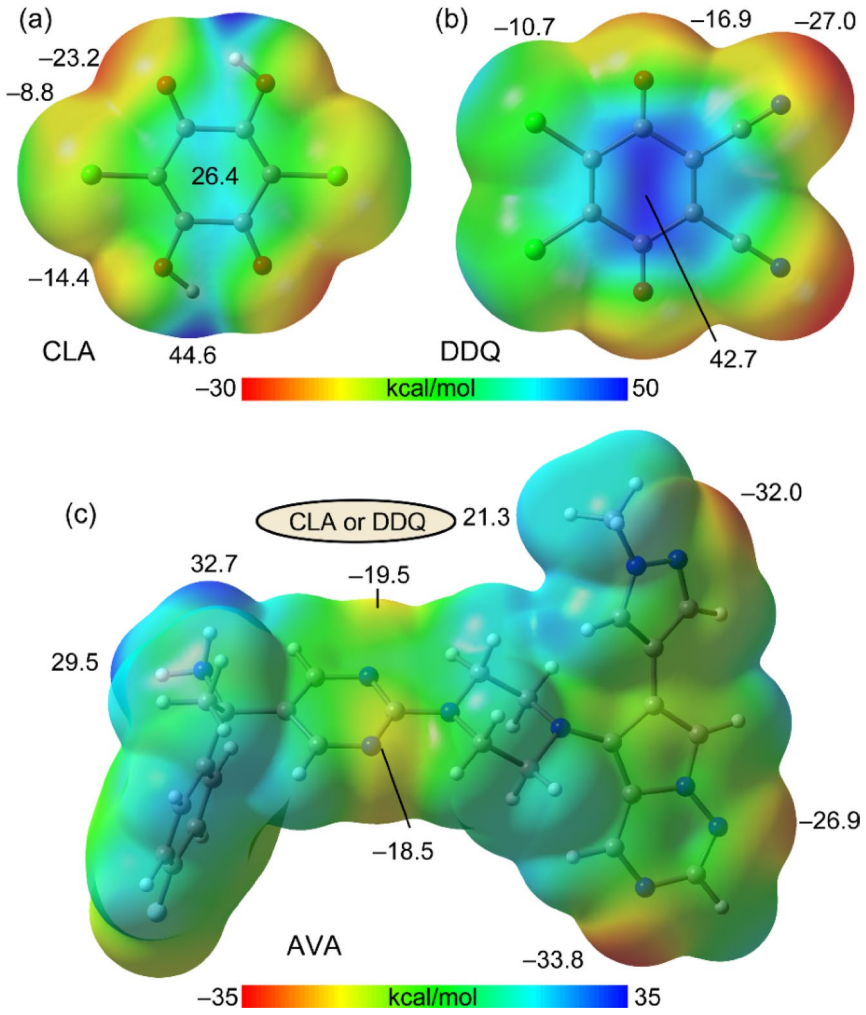

Fig. 5. Molecular Electrostatic Potential (MEP) surfaces mapped onto the 0.001 a.u. electron density isosurface. (**a**) CLA, (**b**) DDQ, and (**c**) AVA. The color scale ranges from -30 to + 50 kcal/mol for the acceptors (**a**, **b**) and − 35 to + 35 kcal/mol for the donor (**c**). Selected local maxima (positive values) and minima (negative values) are indicated on the surfaces in kcal/mol. The ellipse in (**c**) indicates the predicted preferential binding region for the acceptors.

Based on this topographical analysis, the most favorable interaction site on AVA involves the central pyrazine region. The proximity of the electron-deficient amino hydrogens (+32.7 kcal/mol) and the electron-rich pyrazine nitrogen atoms (−18.5/−19.5 kcal/mol) creates an ideal environment for binding the acceptors (DDQ or CLA) through a cooperative mechanism involving both electrostatically enhanced π-stacking interactions and hydrogen bonding. This predicted preferential binding region is highlighted by the ellipse in Fig. 5c.

The extensive conformational search performed using the NCI-CREST method yielded the most stable 1:1 association complexes for AVA with both acceptors. The optimized geometries, shown in Fig. 6, demonstrate a perfect agreement with the predictions made by the MEP surface analysis. In both cases, the acceptor molecules (CLA and DDQ) are positioned directly over the central pyrazine ring of the AVA donor, maximizing the electrostatic complementarity between the electron-rich and electron-deficient regions identified in Fig. 5.

To visualize and categorize the no covalent interactions stabilizing these adducts, we employed the NCI plot index. This method maps the reduced density gradient (RDG) in real space, providing a clear representation of the interaction interfaces. As observed in Fig. 6, both complexes exhibit an extended green isosurface between the aromatic planes, which "embraces" the space between the six-membered rings of the acceptors and the pyrazine ring of AVA. This characteristic feature confirms the formation of a robust π-stacking interaction that serves as the primary stabilizing force.

Beyond π-stacking, the NCI plot analysis reveals specific directional interactions characterized by blue, disk-shaped isosurfaces, which are indicative of strong hydrogen bonds. In the AVA-CLA complex (Fig. 6a), the

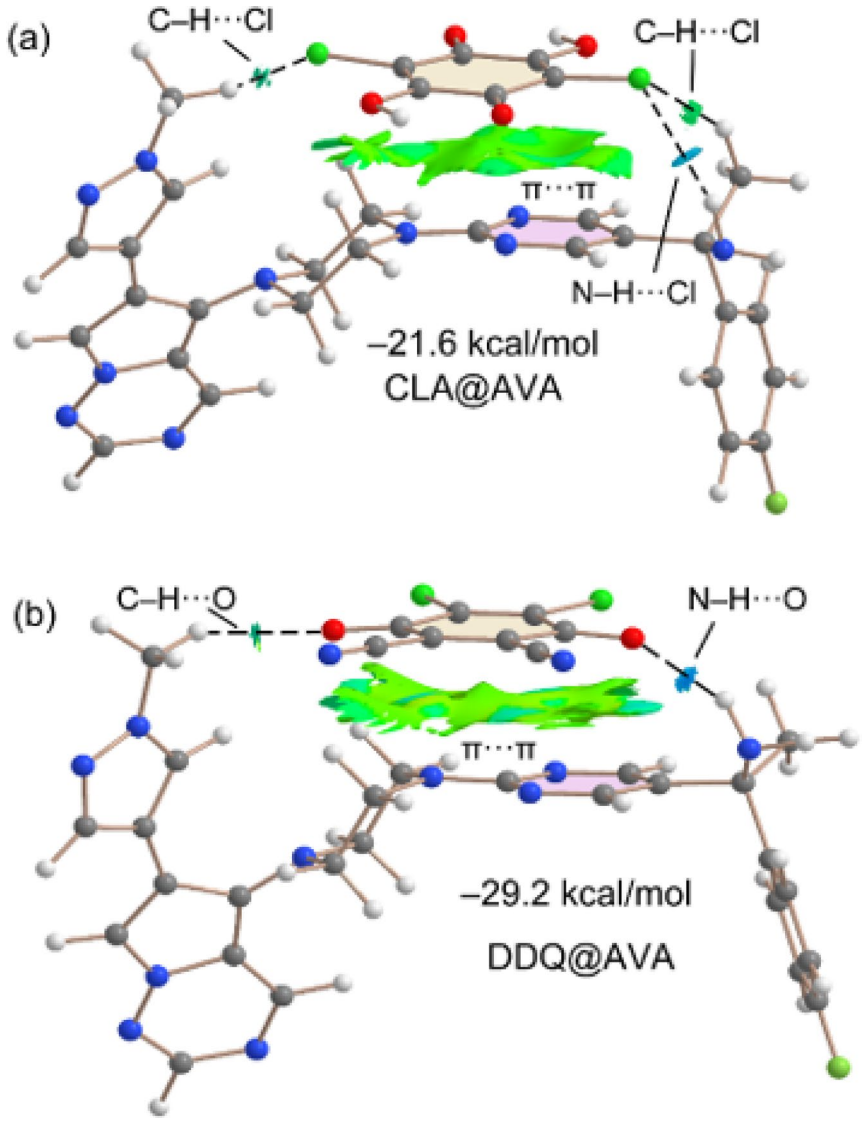

Fig. 6. Optimized geometries of the lowest-energy 1:1 complexes calculated at the PBE0-D3/def2-SVP level of theory: (**a**) CLA@AVA and (**b**) DDQ@AVA. The superimposed NCI plot isosurfaces (isovalue = 0.5 a.u.; color scale -0.04 < sign(lambda_2) rho < 0.04 a.u.) highlight the noncovalent interaction regions. Green surfaces correspond to weak van der Waals/π-stacking interactions, while blue surfaces indicate strong hydrogen bonds (H-bonds). The computed dimerization energies are provided in kcal/mol.

interaction is reinforced by an N–H···Cl hydrogen bond and secondary C-H···Cl contacts. Conversely, in the AVA-DDQ complex (Fig. 6b), the stability is enhanced by a strong N–H···O hydrogen bond involving one of the quinone oxygen atoms, alongside an auxiliary C-H···O contact.

The computed dimerization energies confirm the high stability of these charge transfer complexes, with binding energies of –21.6 kcal/mol for AVA-CLA and –29.2 kcal/mol for AVA-DDQ. These large values support the experimental feasibility of using these reactions for analytical assays. Notably, the interaction with DDQ is significantly stronger (by 7.6 kcal/mol) than with CLA. This energetic trend is fully consistent with our earlier electronic analysis, which showed that DDQ possesses a smaller HOMO–LUMO gap relative to AVA and a more intense positive electrostatic potential over its ring center, thereby leading to a tighter and more stable complex.

Optimization of MW-SPMs conditions

The experimental variables controlling the formation of the CTCs were optimized using the 96-well plate format to establish the optimum conditions for analysis. The effect of acceptor concentration was investigated by varying the amount of DDQ and CLA while keeping the AVA concentration constant. As shown in Fig. 7A, the absorbance at the analytical wavelength (460 nm for DDQ, 520 nm for CLA) increased with acceptor concentration until reaching a relative plateau. This indicates saturation of complex formation, after which further addition of acceptor provides no significant absorbance increase and may lead to increased background absorbance. Based on these patterns, optimal concentrations were selected to ensure maximum analytical response with minimal, efficient reagent use. Accordingly, the optimum concentration of the acceptor, selected for further investigations, was 0.1% (w/v) for both DDQ and CLA.

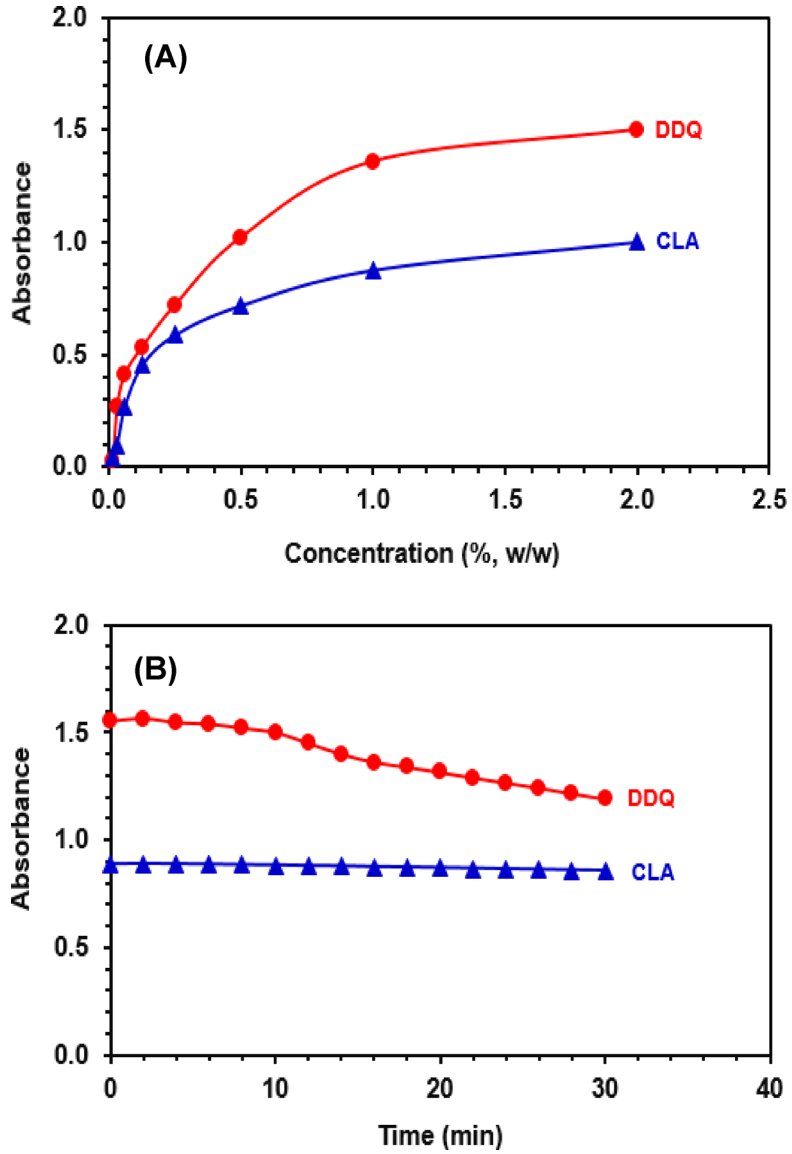

Fig. 7. The effect of acceptor concentration (Panel A) and reaction time (panel B) on the reactions of AVA (50 µg/well) with DDQ and CLA for optimizing the procedures of MW-SPMs for AVA.

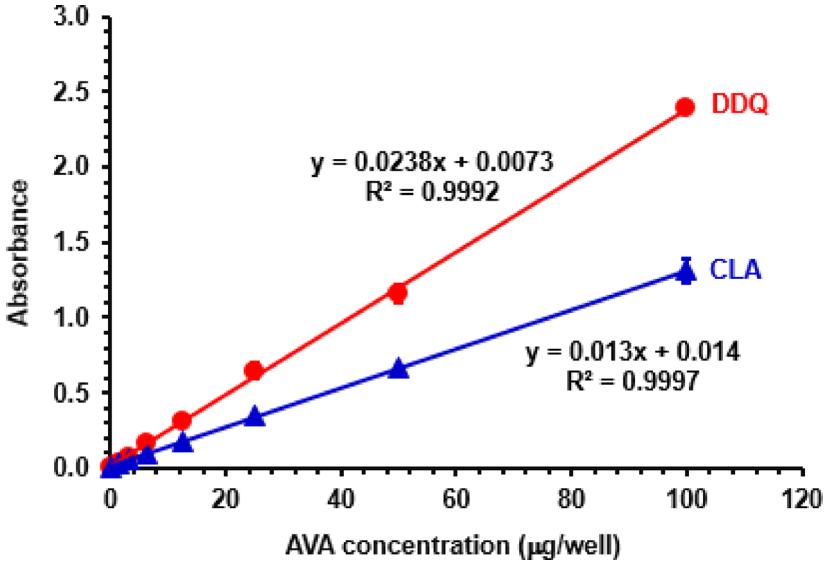

Fig. 8. The calibration curves for the determination of AVA by MW-SPMs via the formation of CTCs with DDQ (Red circle) and CLA (Blue triangle). The linear regression equations and their determination coefficients (R^2) are given on the calibration lines.

Parameter	Value	
	DDQ	CLA
Linear range (µg/well)	3.13–100	6.25–100
Intercept	0.0073	0.014
Slope	0.0238	0.013
Determination coefficient (R^2)	0.9992	0.9997
Limit of detection, LOD (µg/well)	1.5	2.4
Limit of quantitation, LOQ (µg/well)	4.5	7.3

Table 2. The calibration parameters for the determination of AVA by the proposed MW-SPMs via the formation of CTCs with DDQ and CLA.

The kinetics of the reactions were studied by monitoring absorbance over time under the optimized reagent conditions. Both the AVA–DDQ and AVA–CLA complexes formed rapidly at room temperature (Fig. 7B), reaching maximum absorbance instantaneously. Crucially, the absorbance remained stable for at least 30 min, demonstrating the excellent temporal stability of the complexes. This stability is vital for a high-throughput microwell protocol, as it allows for batch processing and plate reading without stringent time constraints, ensuring reproducible results. These optimized conditions—defined acceptor concentrations and a brief, stable reaction time—were adopted for all subsequent method validation and application.

Validation of MW-SPMs

Linearity and sensitivity

Under the optimized conditions, calibration curves were constructed by plotting absorbance against AVA concentration. The AVA–DDQ method exhibited linearity over the range of 3.13–100 µg/well, while the AVA–CLA method was linear from 6.25–100 µg/well (Fig. 8). Both methods demonstrated excellent correlation, with determination coefficients (R^2) of 0.9992 and 0.9997, respectively (Table 2). The higher slope of the DDQ calibration line (0.0238 absorbance units per µg/well) compared to CLA (0.013) indicates greater inherent sensitivity, which is consistent with the higher molar absorptivity of the AVA–DDQ complex (Table 1).The 95% confidence intervals for the slopes were 0.0235–0.0241 (DDQ) and 0.0127–0.0133 (CLA), and for intercepts − 0.002 to + 0.017 (DDQ) and + 0.008 to + 0.020 (CLA). Residual analysis confirmed homoscedasticity and linear model appropriateness, and all validation parameters were aligned with ICH Q2(R2) guidelines[59].

The limits of detection (LOD) and quantification (LOQ) were calculated according to ICH guidelines[59]. The DDQ-based method showed slightly better sensitivity with an LOD of 1.5 µg/well and an LOQ of 4.5 µg/well. The CLA-based method had an LOD of 2.4 µg/well and an LOQ of 7.3 µg/well (Table 2). These values confirm that both MW-SPMs are sufficiently sensitive for the accurate quantification of AVA in pharmaceutical dosage forms.

Precision and accuracy

The precision of the methods was evaluated through intra-day (repeatability) and inter-day (intermediate precision) assays at four concentration levels across the linear range (10, 25, 50, and 80 µg/well). For the DDQ method, intra-day relative standard deviations (RSDs) ranged from 0.6 to 1.8%, and inter-day RSDs from 1.2 to 1.6%. The CLA method showed intra-day RSDs of 1.2–1.8% and inter-day RSDs of 0.8–1.4% (Table 3). All RSD values were well below the commonly accepted limit of 2%, demonstrating excellent method precision.

Accuracy was assessed via recovery studies by spiking known amounts of AVA into sample solutions. The recoveries for the DDQ method ranged from 98.9 to 101.7%, with percentage errors between − 0.5% and 1.7%. For the CLA method, recoveries were between 98.0% and 101.4%, with errors from − 1.2 to 1.4% (Table 3). These results confirm the high accuracy of both methods, with no significant systematic bias.

The excellent precision and accuracy can be attributed to the inherent advantages of the microwell platform: the use of small, controlled reaction volumes minimizes volumetric errors; the parallel processing in 96-well plates enhances reproducibility; and the simplicity and robustness of the one-step CT reaction reduce operational variability.

Robustness

Robustness was evaluated by introducing small, deliberate variations to the optimized procedure (n = 3 per condition). For both DDQ and CLA methods, changing reaction time (5 ± 1 min), temperature (25 ± 2 °C), or acceptor concentration (0.1 ± 0.01% w/v) resulted in recovery values of 98.2–101.5% with RSD < 2.0%, confirming method robustness under routine QC fluctuations.

Analysis of AVA tablets

The validated MW-SPMs were successfully applied to determine AVA in laboratory-prepared tablet formulations. We fully acknowledge the importance of validating analytical methods on commercial pharmaceutical products to enhance practical applicability. However, the commercial tablets of AVA (AYVAKIT™ 50 mg tablets) are not yet approved for marketing in Saudi Arabia, and therefore they are not available for purchase or testing in our region. To overcome this limitation while maintaining scientific rigor, we prepared laboratory tablets that simulate the commercial product as closely as possible. Specifically, we used the same inactive ingredients and followed the qualitative composition stated in the prescribing information document for the reference listed drug, which is publicly available on the FDA website. The laboratory-prepared tablets mimicked the quantitative excipient composition of the commercial AYVAKIT™ 50 mg tablets (copovidone, croscarmellose sodium, magnesium stearate, microcrystalline cellulose, and coating substances). In this context, three independent lab-made batches with different excipient ratios (batch-to-batch variation) were analyzed. The claim percentage was determined to be 100.2% ± 1.5% (DDQ method) and 99.8% ± 1.6% (CLA method). These results validate the successful application of the methods for the precise and accurate quantification of AVA in its tablets.

The ability of the proposed MW-SPMs to quantify AVA in tablets without interference from common pharmaceutical excipients is attributed to two main factors. First, the analytical measurements were conducted in the visible region (460 nm for DDQ and 520 nm for CLA), which is spectrally distant from the UV absorption bands of most inactive ingredients. This ensures the detected signal originates specifically from the colored charge-transfer complex of AVA. Second, the sample preparation utilized acetonitrile as the extraction solvent. Acetonitrile effectively dissolves AVA while leaving many common tablet excipients, such as cellulose derivatives and talc, largely undissolved or insoluble. This selective extraction minimizes co-extraction of interfering matrix components. Together, these factors establish the specificity of the assay, enabling reliable determination of AVA in the presence of typical tablet excipients.

Eco-friendliness and sustainability assessment

The environmental sustainability of the developed AVA MW-SPMs was rigorously evaluated using a suite of ten complementary assessment tools. To ensure a holistic evaluation that avoids the limitations of any single metric, ten complementary assessment tools were employed. Each tool captures a distinct dimension: environmental

AVA concentration (µg/well)	Intra-day ($n = 3$)		Inter-day ($n = 6$)	
	Recovery (% ± RSD)	Error (%)	Recovery (% ± RSD)	Error (%)
DDQ				
10	100.1 ± 1.8	0.1	99.5 ± 1.2	− 0.5
25	101.7 ± 0.9	1.7	98.9 ± 1.4	1.1
50	99.8 ± 1.4	− 0.2	100.2 ± 1.6	0.2
80	100.3 ± 0.6	0.3	99.6 ± 1.5	− 0.4
CLA				
10	99.1 ± 1.2	0.9	100.2 ± 1.4	0.2
25	99.5 ± 1.6	− 0.5	101.4 ± 0.8	1.4
50	98.0 ± 1.8	− 1.2	99.6 ± 1.4	− 0.4
80	100.7 ± 1.4	0.7	98.9 ± 1.1	− 1.1

Table 3. The precision and accuracy of MW-SPMs for the determination of AVA via the formation of CTCs with DDQ and CLA.

impact (AES, AGREE, MoGAPI, AGSA, CaFRI), practical applicability (BAGI, CACI), analytical performance (RAPI), innovation (VIGI), and overall balance (RGB). Together, they provide a non-redundant, multi-dimensional assessment of the method's sustainability, practicality, and analytical rigor.

The benefit of employing multiple complementary metrics lies in their different scopes and weighting systems. For example, AES focuses on penalty points for reagent hazards and waste, while AGREE assesses alignment with the twelve principles of GAC using a color-coded system. MoGAPI evaluates the entire analytical lifecycle, whereas BAGI and CACI focus on practicality and simplicity. Consequently, different tools may yield different scores for the same parameter because they prioritize different aspects (e.g., energy consumption, waste generation, or operator safety). Taken together, they provide a holistic, non-redundant assessment that no single metric can achieve.

Comprehensive reviews have critically evaluated the advantages and limitations of these metric tools, providing guidance for their appropriate application and interpretation[60–64]. Tobiszewski[60] discussed the evolution and practical challenges of greenness metrics, including the trade-offs between simplicity and comprehensiveness. Plotka-Wasylka and Wojnowski[61] compared the complementary use of AGREE and GAPI tools, demonstrating that no single metric is sufficient for holistic assessment. The original GAPI tool and its modifications have been extensively reviewed by Plotka-Wasylka[62], who highlighted its strengths in lifecycle assessment while noting limitations in quantitative precision for comparing closely related methods. For practicality assessment, Manousi et al.[63] evaluated the BAGI tool across diverse analytical applications, identifying key parameters that influence blue scores and discussing scenarios where the tool may require adaptation. The white analytical chemistry framework, including the RGB model, has been comprehensively reviewed by Nowak and Kościelniak[64], who discussed strategies for balancing environmental, performance, and practical criteria while acknowledging the inherent subjectivity in weighting different dimensions. Together, these reviews establish the theoretical and practical foundations for the multi-metric assessment employed in the present study.

Analytical eco-scale (AES) assessment

The AES evaluation yielded an overall score of 90, classifying the method as an excellent green analytical procedure. The penalty point (PP) breakdown was as follows: the amount of solvent and reagents (100 µL acetonitrile + 100 µL reagent) incurred 2 PPs. The hazardous nature of acetonitrile (4 PPs) and the DDQ/CLA reagents (2 PPs) contributed a subtotal of 6 PPs. Energy consumption for the microplate reader and occupational hazards received 0 PPs due to the instrument's low power requirements and the sealed microwell format that minimizes exposure. Waste production (< 1 mL per sample) and treatment (absence of dedicated protocols) accounted for 1 PP and 3 PPs, respectively. The total of 10 PPs (100—10 = 90) confirms the method's minimal environmental burden.

Multi-Metric profile and discussion

A comprehensive evaluation using multiple metrics further delineated the strengths of the MW-SPMs, with key results summarized in Fig. 9.The multi-metric assessment (Fig. 9) confirmed the method's excellent greenness (AGREE: 0.79; MoGAPI: 84%; AGSA: 87.5%), high practicality (BAGI: 80; CACI: 86), outstanding analytical performance (RAPI: 87.5), and exceptional whiteness (RGB Index: 94.2%), positioning the developed MW-SPMs as modern, sustainable, and high-performance alternatives to traditional chromatographic methods for AVA analysis.

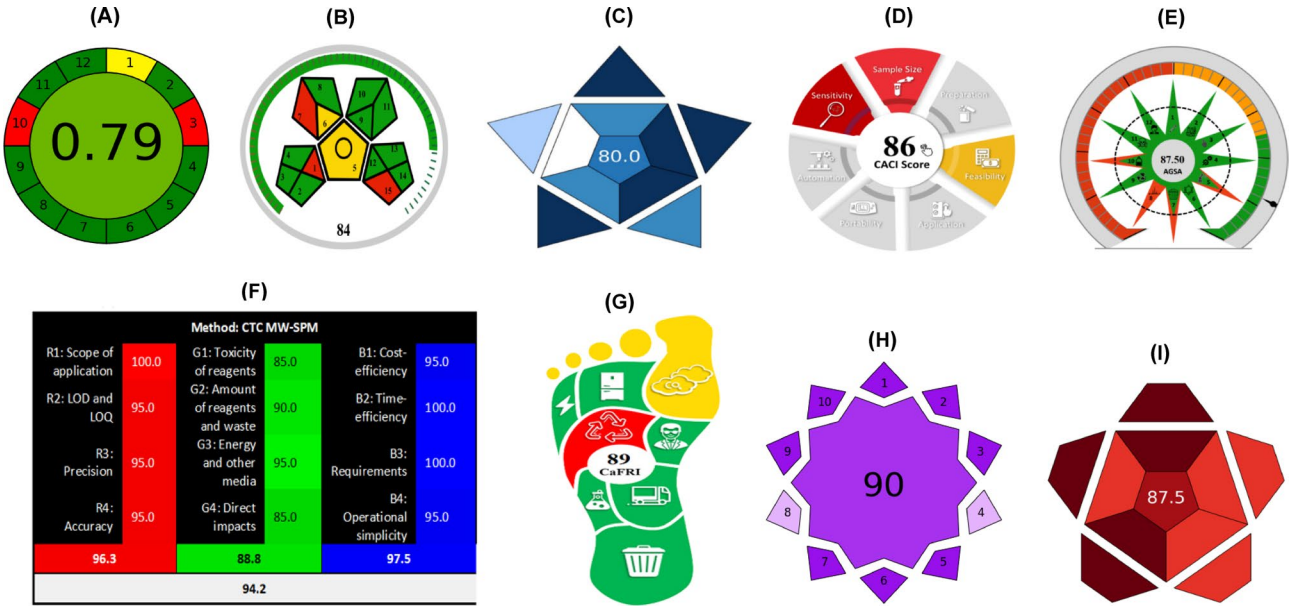

Fig. 9. Multi-metric evaluation pictograms: (**A**) AGREE, (**B**) MoGAPI, (**C**) BAGI, (**D**) CACI, (**E**) AGSA, (**F**) RGB, (**G**) CaFRI, (**H**) VIGI, (**I**) RAPI.

Contribution to sustainable development goals

The alignment of the AVA MW-SPMs with broader global sustainability objectives was mapped against relevant United Nations Sustainable Development Goals (SDGs), as detailed in Table 6.

- *SDG 3 (Good Health and Well-Being)*: Supported by providing robust, reliable tools for pharmaceutical quality assurance of AVA.
- SDGs 4 & 17 (Quality Education & Partnerships): Facilitated by the method's simplicity and low instrumental demands, which ease technology transfer and training.
- SDG 12 (Responsible Consumption and Production): Directly advanced through drastic reductions in solvent and reagent consumption.
- SDGs 13 & 15 (Climate Action and Life on Land): Contributed to via a minimized carbon footprint (CaFRI), reduced hazardous waste generation, and lower overall environmental burden.

This SDG mapping contextualizes the analytical advancement within a framework of global responsibility, underscoring the method's contribution beyond the laboratory.

Multi-metric comparative assessment

While a fully quantitative comparative assessment using AGREE, MoGAPI, BAGI, and RGB metrics would require dedicated calculation for each published method based on detailed experimental protocols, a qualitative comparison based on method characteristics reveals consistent advantages of the proposed MW-SPMs, as shown in Table 7.

The proposed MW-SPMs operate with minimal solvent consumption (200 µL/well), high throughput (~ 500 samples/h), low energy requirements (microplate reader), and generate minimal waste. In contrast, reported HPLC–UV methods [6–10] consume 15–20 mL of mobile phase per sample, achieve throughput of only 5–15 samples/h, require high-pressure pumps and prolonged column equilibration, and generate substantial organic waste. Spectrofluorimetric methods[15–17] consume 2–3 mL of solvent per sample, require temperature-controlled derivatization steps (15–30 min per batch), and achieve throughput of approximately 5 samples/h.

Based on these characteristics, the proposed MW-SPMs are expected to achieve superior AGREE, MoGAPI, BAGI, and RGB scores compared to both HPLC–UV and spectrofluorimetric methods, primarily due to drastic reductions in solvent consumption, waste generation, analysis time, and energy requirements. This positions the MW-SPMs as a genuinely greener, more practical, and higher-throughput alternative for routine AVA quality control (Table 4).

Comparative method evaluation

The performance characteristics of the developed MW-SPMs were compared against published spectrofluorimetric and HPLC–UV methods for AVA analysis (Table 5). This comparative evaluation highlights

Eco-Scale score parameters	Penalty points (PPs)
Amount of solvent/reagent	
Solvent: < 1 mL (mL (g) per sample)	1
Reagent: < 1 mL (mL (g) per sample)	1
	Σ = 2
Hazard of solvent/reagent	
Solvent: acetonitrile	4
Reagent: DDQ and CLA	2
	Σ = 6
Instrument: Energy used (kWh per sample)	
Microplate reader	0
	Σ = 0
Occupational hazardous	
Analytical process hermetic	0
Emission of vapors and gases to the air	0
	Σ = 0
Waste	
Production (< 1 mL (g) per sample)	1
Treatment (No treatment involved)	3
	Σ = 4
Total PPs	10
Eco-Scale score	90

Table 4. Analytical Eco-Scale for assessing the eco-friendliness of the proposed MW-SPMs for the determination of AVA via the formation of CTCs with DDQ and CLA.

the distinctive advantages of the proposed approach across key parameters of analytical efficiency, sustainability, and practicality.

Analytical range and sensitivity
The proposed MW-SPMs offer wide linear dynamic ranges (3.13–100 and 6.25–100 µg/well for DDQ and CLA, respectively), which comfortably encompass the determination of AVA quantity in pharmaceutical tablets. While the reported spectrofluorimetric and some HPLC methods demonstrate lower LOQ values (0.007–0.09 µg mL^{-1}), achieving superior sensitivity for trace analysis in biological matrices like plasma, their linear ranges are considerably narrower. The LOQ values of the MW-SPMs (4.5 and 7.3 µg/well) are fully fit-for-purpose for the direct quantification of AVA in tablet dosage forms, where the analyte is present at milligram-per-tablet levels.

Throughput and analytical efficiency
The most pronounced advantage of the proposed MW-SPMs is their exceptional sample throughput. Both the DDQ- and CLA-based methods enable the analysis of ~ 500 samples per hour. This rate is orders of magnitude higher than those of reported spectrofluorimetric methods (~ 5 samples/h) and all listed HPLC–UV methods (range: 5–15 samples/h). This unparalleled throughput stems directly from the 96-well microplate format, which facilitates the parallel processing of dozens of samples simultaneously, a feature absent in sequential analytical techniques.

Greenness and operational footprint
A critical differentiator is the inherent greenness of the MW-SPM platform. The methodology circumvents the high solvent consumption intrinsic to HPLC, which typically requires milliliters of organic solvent per sample (15–20 mL) for mobile phase preparation and column equilibration. In contrast, the MW-SPMs consume only 200 µL of total reaction volume per well, resulting in minimal solvent use and waste generation. As shown in Table 6, the AGREE scores for HPLC and spectrofluorimetric methods (~ 0.30–0.50) are substantially lower than the score achieved by the proposed MW-SPMs (0.79), confirming the superior greenness of the microwell platform.

Trade-offs summary
Spectrofluorimetric and HPLC–UV methods achieve lower LOQ values suitable for trace analysis but sacrifice throughput (5–15 samples/h) and greenness (high solvent consumption). In contrast, the proposed MW-SPMs offer adequate sensitivity for tablet analysis (fit-for-purpose given the milligram-per-tablet drug content) while providing exceptional throughput (~ 500 samples/h) and excellent greenness (AGREE 0.79). Thus, our method is optimally engineered for routine quality control in industrial settings, where speed and sustainability are prioritized over trace-level sensitivity (Table 7).

Instrumentation and practicality
The proposed methods replace sophisticated, costly, and maintenance-intensive HPLC systems with a standard microplate reader, a common and robust instrument in modern analytical laboratories. This shift eliminates the need for high-pressure pumps, specialized columns, and extensive method development and equilibration times. The simplicity of the direct charge-transfer complex formation, combined with automated plate reading, translates to a method with lower capital cost, reduced technical skill requirements, and enhanced operational robustness for high-volume routine analysis.

Conclusion of comparison
In summary, the proposed MW-SPMs present a compelling alternative to existing methods for the quality control of AVA in pharmaceuticals. They uniquely combine high-throughput capability, adequate sensitivity for dosage form analysis, superior environmental sustainability, and exceptional practical efficiency. While chromatographic and highly sensitive spectrofluorimetric methods retain their necessity for specific applications such as metabolic studies or trace bioanalysis, the MW-SPMs are optimally engineered for the demands of rapid, cost-effective, and green routine analysis in industrial settings.

Conclusion

This study successfully established and validated two innovative, sustainable, and efficient MW-SPMs for the determination of AVA in its tablet dosage form. By exploiting the CT complexation of AVA with the π-acceptors DDQ and CLA within a 96-well plate platform, the developed methods harness the combined advantages of spectrophotometric simplicity, miniaturization, and parallel processing. The CT reactions were thoroughly characterized, with DFT calculations providing molecular-level insights into the 1:1 stoichiometry and the non-covalent interactions—primarily π-stacking and hydrogen bonding—that stabilize the complexes. The optimized MW-SPMs fulfilled all standard validation criteria, demonstrating suitable linearity, sensitivity, accuracy, and precision for the intended purpose of routine quality control. The most significant advancement lies in the holistic performance profile of these methods. A rigorous multi-metric sustainability assessment, encompassing ten complementary evaluation tools, unequivocally validated their alignment with the principles of GAC. The methods achieved outstanding scores in greenness (e.g., AES = 90, AGREE = 0.79), practicality (BAGI = 80, CACI = 86), and analytical performance (RAPI = 87.5), culminating in a high White Index of 94.2% (Red: 96.3%, Green: 88.8%, Blue: 97.5%). This confirms the successful harmonization of analytical rigor, environmental responsibility, and operational feasibility. Furthermore, the methods offer transformative practical benefits: an exceptional throughput of approximately 500 samples per hour, a drastic reduction in solvent consumption and

SDG (Figure)	Goal	Alignment of the proposed AVA–CTC method
SDG 3 	Good health and well-being	Ensures therapeutic quality by providing a robust, highly selective, and validated quality control method for AVA. This contributes to better patient outcomes and public health by confirming the quality and safety of this critical anti-cancer drug
SDG 4 	Quality education	Demonstrates practical application of charge-transfer complexation in pharmaceutical analysis. Serves as an accessible teaching model for spectrophotometric method development and sustainable analytical chemistry
SDG 5 	Gender equality	Simple analytical workflow and low instrumentation requirements support inclusive participation in laboratory training and research. Reduces dependence on highly specialized expertise, facilitating broader access to analytical practice
SDG 7 	Affordable and clean energy	Spectrophotometric detection avoids energy-intensive chromatographic systems. Short analysis time and plate-based measurements reduce overall instrument operation time
SDG 9 	Industry, innovation and infrastructure	Promotes sustainable industrialization by deploying a novel, resource-efficient, and highly practical analytical method alternative to separation-based techniques. The method's high practicality is confirmed by a BAGI score of 82.5, along with high scores in AGSA and CaFRI
SDG 11 	Sustainable cities and communities	Minimal solvent consumption and reduced waste generation support sustainable laboratory practices in urban settings. Compact instrumentation footprint lowers laboratory space and infrastructure demands
SDG 12 	Responsible consumption and production	Uses small volumes of solvent and reagents per analysis. Eliminates continuous solvent consumption associated with chromatographic mobile phases. Optimized reagent utilization minimizes chemical waste generation
SDG 13 	Climate action	Reduced energy demand and solvent use contribute to lower environmental impact compared with conventional chromatographic methods. Supports climate-conscious analytical practices through simplified workflows
SDG 15 	Life on land	Minimization of hazardous waste supports protection of terrestrial ecosystems. Reduced chemical consumption contributes to lower land-based waste disposal
SDG 17 	Partnerships for the goals	Simple and cost-effective methodology facilitates inter-laboratory adoption and collaboration. Supports harmonization of sustainable analytical practices across academic and industrial quality-control laboratories

Table 5. Alignment of the proposed MW-SPMs with UN sustainable development Goals (SDGs).

Method	Sample matrix	Linear range (µg mL^{-1})	LOQ (µg mL^{-1})	Throughput (samples/h)	Solvent/ sample(mL)	Greenness-Speed-Sensitivity Trade -off	Ref
MW-SPM (using DDQ)	Tablets	3.13-100[b]	4.5[b]	500	0.2	Excellent (high throughput, good greenness, adequate sensitivity)	PS
MW-SPM (using CLA)	Tablets	6.25-100[b]	7.3[b]	500	0.2	Excellent (high throughput, good greenness, adequate sensitivity)	PS
Spectrofluorimetry (Derivatization with NBD-Cl)	Tablets, plasma	0.08–0.9	0.02	5	2.5	Poor (high sensitivity, low throughput, moderate greenness)	15
Spectrofluorimetry (Derivatization with DHID)	Tablets, plasma	0.4–4	0.1	5	3	Poor (high sensitivity, low throughput, moderate greenness)	16
Spectrofluorimetry (micelle formation with SDS)	Tablets, plasma	0.02–0.4	0.09	5	3	Poor (high sensitivity, low throughput, moderate greenness)	17
HPLC–UV	Bulk, tablets	5–30	1.27	8	15	Poor (moderate sensitivity, very low throughput, low greenness)	6
HPLC–UV	Bulk, tablets	0.5–12	0.8	10	15	Poor (moderate sensitivity, low throughput, low greenness)	7
HPLC–UV	Tablets	4–20	0.6	15	15	Poor (moderate sensitivity, low throughput, low greenness)	8
HPLC–UV	Bulk	25–150	8.8	5	20	Poor (low sensitivity, very low throughput, low greenness)	9
HPLC–UV	Bulk, tablets	0.05–0.15	0.007	12	20	Poor (high sensitivity but very low throughput and greenness)	10

Table 6. Comparative evaluation of the analytical performance of the proposed MW-SPMs with the reported methods for the determination of AVA[a]. [a] MW-SPM: microwell spectrophotometric method, AVA: avapritinib, DDQ: 2,3-dichloro-5,6-dicyano-1,4-benzoquinone, CLA: chloranilic acid, NBD-Cl: 4-chloro-7-nitrobenzofurazan, DHID: 2,2-Dihydroxyindane-1,3-Dione, SDS: sodium dodecyl sulfate, HPLC–UV: high performance liquid chromatography with ultraviolet detection, PS: present study. [b]Concentrations are givenin µg/well (µg/100µL).

waste generation (200 µL/well), and the use of widely available and cost-effective microplate instrumentation. This positions the MW-SPMs as a compelling, modern alternative to resource-intensive chromatographic and low-throughput spectrofluorimetric techniques for industrial quality control laboratories. In conclusion, the proposed MW-SPMs represent a significant step forward in the eco-friendly, high-throughput analysis of targeted anticancer therapies. They provide a reliable, sustainable, and economically advantageous platform for ensuring the pharmaceutical quality of AVA, contributing meaningfully to the broader goals of sustainable science and global health. Future studies should extend validation to commercial AVA products and biological matrices to further demonstrate the method's versatility. Additionally, techniques such as mass spectrometry or FTIR spectroscopy could provide direct structural evidence for the charge-transfer complexes, complementing the indirect evidence (Job's method, Benesi-Hildebrand plots, and DFT calculations) presented in this work.

Analytical technique	AGREE score	MoGAPI (%)	BAGI score	RGB (Whiteness %)	Ref
Proposed MW-SPM	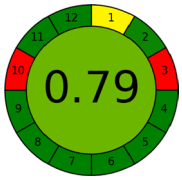			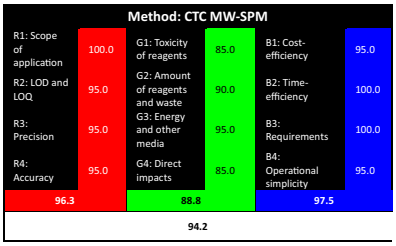	PS
Spectro-fluorimetry (NBD-Cl)	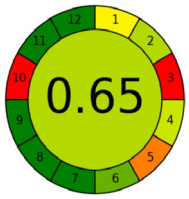	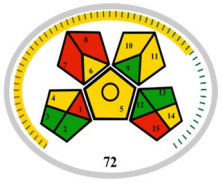		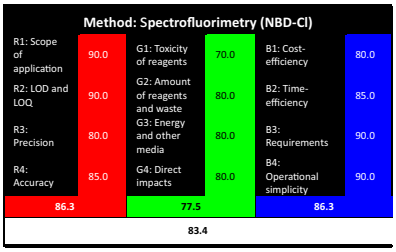	15
Spectro-fluorimetry (DHID)	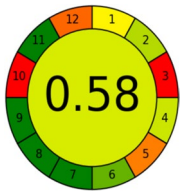	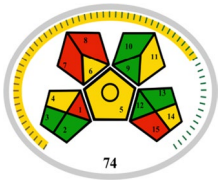		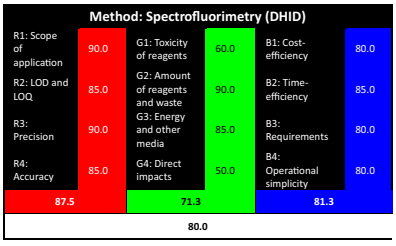	16
Spectro-fluorimetry (SDS)		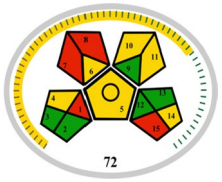		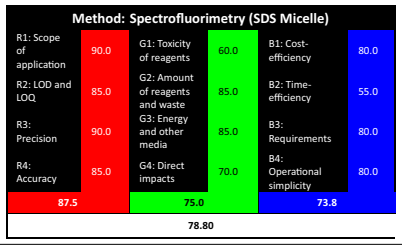	17
HPLC–UV	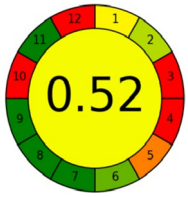	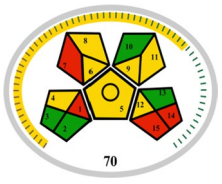		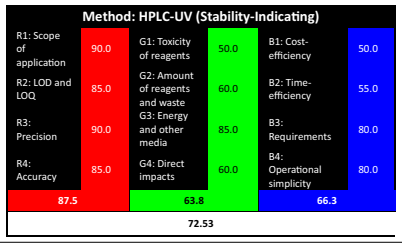	6
HPLC–UV	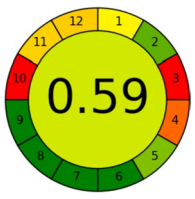	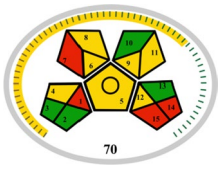		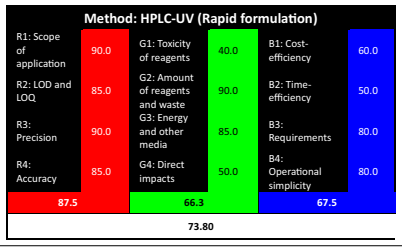	7
HPLC–UV	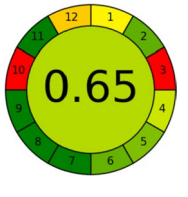	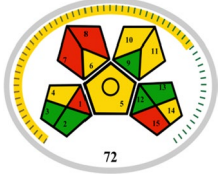		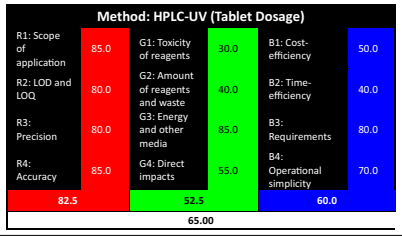	8

Continued

Analytical technique	AGREE score	MoGAPI (%)	BAGI score	RGB (Whiteness %)	Ref
HPLC–UV	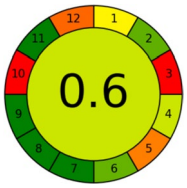	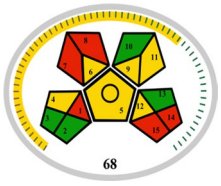		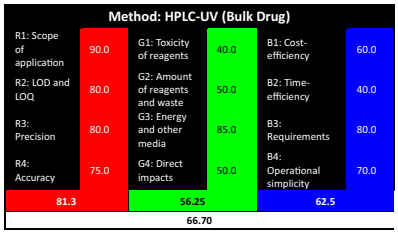	9
HPLC–UV	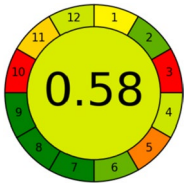			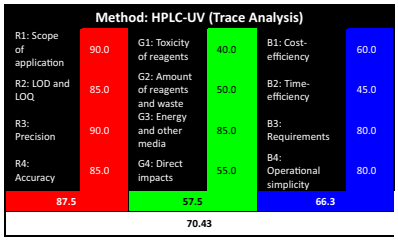	10

Table 7. Multi-metric evaluation of the proposed and reported methods for AVA using AGREE, MoGAPI, BAGI, and RGB metrics.

Data availability

All data generated or analyzed during this study are included in this article. Any additional datasets are available from the corresponding author upon reasonable request.

Received: 8 March 2026; Accepted: 30 April 2026
Published online: 21 May 2026

References

1. Teuber, A. et al. Avapritinib-based SAR studies unveil a binding pocket in PDGFRA and KIT. *Nat. Commun.* **15**, 1234 (2024).
2. Sandow, L. et al. Avapritinib treatment of aggressive systemic mastocytosis. *Leuk. Res.* **134**, 107529 (2024).
3. FDA. Ayvakit (avapritinib) prescribing information (Blueprint Medicines Corporation (2022). https://www.accessdata.fda.gov/drugsatfda_docs/label/2020/212608s000lbl.pdf
4. Rasagna, P. et al. Development and validation of analytical RP-HPLC method for Avapritinib. *Pharm. Growth J.* **14**, 100–107 (2024).
5. Yang, Y. D. et al. Absolute configuration and chiroptical properties of flexible drug Avapritinib. *Pharmaceuticals* **18**, 833 (2025).
6. Mishra, S. et al. A validated stability indicating RP-HPLC method for estimation of avapritinib in bulk and tablet dosage form. *Int. J. Appl. Pharm.* **14**, 95–101 (2022).
7. Suresh, C. H. V. et al. A new analytical method development and validation of estimation of avapritinib by RP-HPLC. *Int. J. Multidiscipl. Res. Growth Eval.* **4**, 175–182 (2023).
8. Babu, R. S. et al. RP-HPLC method development and validation for the estimation of Avapritinib in bulk form and marketed pharmaceutical dosage form. *J. Pharm. Anal.* **14**, 456–462 (2024).
9. Shaik, R. B. et al. LC–MS/MS profiling of stress-induced degradation products of Avapritinib and development of a stability-indicating HPLC method for its quantification and impurity analysis. *Methods Objects Chem. Anal.* **20**, 1–12 (2025).
10. Singh, T. G. et al. Analytical method development and validation of avapritinib by RP-HPLC method. *World J. Pharm. Pharm. Sci.* **9**, 1834–1840 (2020).
11. Attwa, M. W. et al. Assessment of the metabolic stability of Avapritinib in human liver microsomes using a fast and green UPLC–MS/MS method: Screening for structural alarms associated with metabolic lability and in silico toxicity. *Anal. Methods.* **17**, 7431–7443 (2025).
12. Kumari, G. K. & Rambabu, K. Bio-analytical method development and validation for avapritinib in rat plasma by LC–MS/MS. *J. Pharm. Sci. Res.* **13**, 134–137 (2021).
13. Xu, X. et al. Development and validation of the quantitative determination of avapritinib in rat plasma by a bioanalytical method of UPLC–MS/MS. *Arab. J. Chem.* **14**, 103152 (2021).
14. Saraya, R. E. et al. Applicability of fluorescamine as a fluorogenic reagent for highly sensitive fluorimetric analysis of the tyrosine kinase inhibitor (avapritinib) in pharmaceuticals and biological samples. *Luminescence* **38**, 1632–1638 (2023).
15. Salman, B. I. et al. A green bioanalytical spectrofluorimetric approach for estimation of avapritinib anti-tumor drug; application to quality control and clinical studies. *Bioanalysis* **17**, 31–40 (2025).
16. Salman, B. I. Quantification of the anticancer drug avapritinib in human plasma using 2, 2-dihydroxyindane-1, 3-dione: Application to a pharmacokinetic study. *J. Anal. Chem.* **80**, 675–683 (2025).
17. Salman, B. I. et al. A new green fluorimetric micelle complexation approach for reduction of the consumed solvent and quantification of avapritinib in biological fluids. *RSC Adv.* **14**, 10445–10451 (2024).
18. Eldin, A. B. et al. A. green analytical chem.: Opportunities for pharmaceutical quality control. *Anal. Chem.* **71**, 861–871 (2019).
19. Garg, V. K., et al. *Green Chemistry Approaches to Environmental Sustainability Status: Challenges and Prospective.* Elsevier (2024).
20. Varu, H. L. et al. An Expeditious spectrophotometric estimation of memantine hydrochloride by facile derivatization using N. *N-dimethyl aniline. J. Anal. Chem.* **77**, 1433–1439 (2022).
21. Varu, H. L. et al. Molecular iodine mediated spectrophotometric determination of tolfenamic acid in pharmaceutical and veterinary formulations. *J. Anal. Chem.* **78**, 687–693 (2023).
22. Varu, H. L. et al. Kinetic spectrophotometric determination of memantine hydrochloride based on the formation of its dinitrochlorobenzene adduct. *J. Anal. Chem.* **79**, 1431–1438 (2024).
23. Wang, P. G. (ed.) *High-Throughput Analysis in the Pharmaceutical Industry.* CRC Press (2019).

24. Welch, C. J. High throughput analysis enables high throughput experimentation in pharmaceutical process research. *React. Chem. Eng.* **4**, 1895–1911 (2019).
25. Liu, G. & Lin, J.-M. Microplate-based assays: The future of pharmaceutical analysis. *Trends Anal. Chem.* **85**, 43–48 (2016).
26. Singh, P. & Singh, B. Microwell spectrophotometry: A green analytical technique for pharmaceutical analysis. *J. Pharm. Anal.* **7**, 203–208 (2017).
27. Darwish, I. A. et al. Evaluation of 4-fluoro-7-nitrobenzofurazan as a dual-function chromogenic and fluorogenic probe for tulathromycin and its innovative utility for development of two eco-friendly and high-throughput microwell assays for analysis of pharmaceutical formulations. *Spectrochim. Acta A Mol. Biomol. Spectrosc.* **325**, 125079 (2025).
28. Darwish, I. A. & Alzoman, N. Z. Green and versatile high-throughput microwell oxidation-based spectrophotometric methods for determination of galidesivir in capsules. *J. AOAC Int.* **107**, 727–734 (2024).
29. Darwish, I. A. & Alsalhi, M. S. Development of two green and high-throughput microwell spectrometric platforms for determination of reboxetine, the first FDA-approved selective noradrenaline reuptake inhibitor antidepressant drug. *J. AOAC Int.* **107**, 912–920 (2024).
30. Rezvan, V. H. Charge transfer complexes: A review survey. *Results Chem.* **17**, 102600 (2025).
31. Baharfar, M. et al. Charge-transfer complexes: Fundamentals and advances in catalysis, sensing, and optoelectronic applications. *Adv. Mater.* **36**, 2406083 (2024).
32. Rezvan, V. H. A review of drug analysis using charge transfer complexes. *Chem. Nanochem.* **2**, 11–27 (2023).
33. Darwish, I. A. & Alzoman, N. Z. Development of green and high throughput microplate reader-assisted universal microwell spectrophotometric assay for direct determination of tyrosine kinase inhibitors in their pharmaceutical formulations irrespective the diversity of their chemical structures. *Molecules* **28**, 4049 (2023).
34. Hosny, N. M. et al. A. microwell-based spectrophotometric analysis of pemigatinib via formation of charge transfer complexes: Eco-friendly and high-throughput methods. *J. Chem. Res.* **49**, 1–14 (2025).
35. Darwish, I. A. et al. A one-step green microwell spectrophotometric assay for the determination of certain new chemotherapeutic drug formulations. *J. AOAC Int.* **107**, 903–911 (2024).
36. Alsharif, M. A. et al. DDQ as a versatile and easily recyclable oxidant: A systematic review. *RSC Adv.* **11**, 29826–29858 (2021).
37. Aljaber, K. A. et al. Spectrophotometric study of charge-transfer complexes of ruxolitinib with chloranilic acid and 2,3-dichloro-5,6-dicyano-1,4-benzoquinone: An application to the development of a green and high-throughput microwell method for quantification of ruxolitinib in its pharmaceutical formulations. *Molecules* **28**, 7877 (2023).
38. Singh, N. & Ahmad, A. Spectrophotometric studies on the charge-transfer interaction between p-nitroaniline with chloranilic acid as π–acceptor in different polar solvents. *J. Mol. Struct.* **1127**, 257–265 (2017).
39. Benesi, H. A. & Hildebrand, J. H. A spectrophotometric investigation of the interaction of iodine with aromatic hydrocarbons. *J. Am. Chem. Soc.* **71**, 2703–2707 (1949).
40. Job, P. Formation and stability of inorganic complexes in solution. *Ann. Chim.* **9**, 113–134 (1928).
41. Frisch, M. J. *et al. Gaussian 16, Revision C.01*. Gaussian, Inc., Wallingford, CT, USA, (2016).
42. Adamo, C. & Barone, V. Toward reliable density functional methods without adjustable parameters: The PBE0 model. *J. Chem. Phys.* **110**, 6158–6170 (1999).
43. Grimme, S. et al. A consistent and accurate Ab initio parametrization of density functional dispersion correction (DFT-D) for the 94 elements H-Pu. *J. Chem. Phys.* **132**, 154104 (2010).
44. Weigend, F. & Ahlrichs, R. Balanced basis sets of split valence, triple zeta valence and quadruple zeta valence quality for H to Rn: Design and assessment of accuracy. *Phys. Chem. Chem. Phys.* **7**, 3297–3305 (2005).
45. Pracht, P. et al. Automated exploration of the low-energy chemical space with fast quantum chemical methods. *Phys. Chem. Chem. Phys.* **22**, 7169–7192 (2020).
46. Boys, S. F. & Bernardi, F. The calculation of small molecular interactions by the differences of separate total energies. Some procedures with reduced errors. *Mol. Phys.* **19**, 553–566 (1970).
47. Johnson, E. R. et al. Revealing noncovalent interactions. *J. Am. Chem. Soc.* **132**, 6498–6506 (2010).
48. Keith, T. A. *AIMAll, Version 19.10.12*. TK Gristmill Software, Overland Park, KS, USA, (2019).
49. Gałuszka, A. et al. Analytical Eco-Scale for assessing the greenness of analytical procedures. *TrAC Trends Anal. Chem.* **37**, 61–72 (2012).
50. Pena-Pereira, F. et al. AGREE—Analytical GREEnness metric approach and software. *Anal. Chem.* **92**, 10076–10082 (2020).
51. Mansour, F. R. et al. Modified GAPI (MoGAPI) tool and software for the assessment of method greenness: Case studies and applications. *Analytica* **5**, 451–457 (2024).
52. Manousi, N. et al. Blue applicability grade index (BAGI) and software: A new tool for the evaluation of method practicality. *Green Chem.* **25**, 7598–7604 (2023).
53. Mansour, F. R. et al. Click analytical chemistry index as a novel concept and framework, supported with open source software to assess analytical methods. *Adv. Sample Prep.* **14**, 100164 (2025).
54. Nowak, P. M. et al. White analytical chemistry: An approach to reconcile the principles of green analytical chemistry and functionality. *TrAC Trends Anal. Chem.* **138**, 116223 (2021).
55. Mansour, F. R. et al. Analytical green star area (AGSA) as a new tool to assess greenness of analytical methods. *Sustain. Chem. Pharm.* **46**, 102051 (2025).
56. Mansour, F. R. & Nowak, P. M. Introducing the carbon footprint reduction index (CaFRI) as a software-supported tool for greener laboratories in chemical analysis. *BMC Chem.* **19**, 121 (2025).
57. Fuente-Ballesteros, A. et al. Violet innovation grade index (VIGI): A new survey-based metric for evaluating innovation in analytical methods. *Anal. Chem.* **97**, 6946–6955 (2025).
58. Nowak, P. M. et al. Red analytical performance index (RAPI) and software: The missing tool for assessing methods in terms of analytical performance. *Green Chem.* **27**, 5546–5553 (2025).
59. ICH. *Validation of analytical procedures Q2(R2)* International Council for Harmonisation (2022).
60. Tobiszewski, M. Metrics for green analytical chemistry. *Anal. Methods* **8**, 2993–2999 (2016).
61. Plotka-Wasylka, J. & Wojnowski, W. Complementary green analytical procedure index and AGREE for greenness assessment of analytical methods. *Talanta* **233**, 122544 (2021).
62. Plotka-Wasylka, J. A new tool for the evaluation of the analytical procedure: Green analytical procedure index. *Talanta* **181**, 204–209 (2018).
63. Manousi, N., Zachariadis, G. A. & Anthemidis, A. Blue applicability grade index: Practical applications and limitations in pharmaceutical analysis. *Green Chem.* **26**, 456–468 (2024).
64. Nowak, P. M. & Kościelniak, P. White analytical chemistry: Strategies and perspectives for balancing greenness and functionality. *TrAC Trends Anal. Chem.* **147**, 116517 (2022).

Acknowledgements

The authors extend their appreciation to the Ongoing Research Funding program, (ORF-2026-2124), King Saud University, Riyadh, Saudi Arabia, for funding this work.

Author contributions

I.A.D., A.M.A., and M.S.A. conceived and designed the study. A.M.A., W.A., and M.S.A. performed the experimental lab work and data collection. A.F. performed the computational DFT analysis and molecular modeling. W.M.O. conducted the comprehensive greenness and sustainability multi-metric assessments. I.A.D., W.A., W.M.O., and A.M.A. analyzed the data and wrote the main manuscript text. I.A.D. provided the resources, secured the funding, and supervised the entire project. All authors reviewed and approved the final manuscript.

Funding

This research was funded by the Ongoing Research Funding program, (ORF-2026–2124), King Saud University, Riyadh, Saudi Arabia.

Declarations

Competing interests

The authors declare no competing interests.

Additional information

Supplementary Information The online version contains supplementary material available at https://doi.org/10.1038/s41598-026-51872-6.

Correspondence and requests for materials should be addressed to W.M.O.

Reprints and permissions information is available at www.nature.com/reprints.

Publisher's note Springer Nature remains neutral with regard to jurisdictional claims in published maps and institutional affiliations.